Journal of Geosciences, 61 (2016), 221–237 DOI: 10.3190/jgeosci.215

Original paper

U–Pb zircon ages from Permian volcanic rocks and tonalite of the Northern Veporicum (Western Carpathians)

Anna VOZÁROVÁ[1*], Nickolay RODIONOV[2], Jozef VOZÁR[3], Elena LEPEKHINA[2], Katarína ŠARINOVÁ[1]

[1] *Comenius University Bratislava, Faculty of Natural Sciences, Department of Mineralogy and Petrology, Mlynská dolina, Ilkovičova 6, 84215 Bratislava, Slovak Republic; vozarova@fns.uniba.sk*

[2] *Centrum Isotopic Research, All-Russian Geological Research Institute (VSEGEI), Sredny prospekt 74, 199 106 St.-Petersburg, Russia*

[3] *Earth Science Institute of Slovak Academy of Sciences, Dúbravská cesta 9, 840 05 Bratislava, Slovak Republic*

**Corresponding author*

U–Pb dating (SHRIMP) of magmatic zircons from the Northern Veporicum Permian volcanics of the Ľubietová Group yielded concordia ages of 273 ± 6 Ma and 279 ± 4 Ma. Both zircon ages correspond to the Cisuralian Epoch in the time span of Kungurian Stage. The 272 ± 4 Ma U–Pb zircon age, determined on the volcanic dyke cutting the neighbouring crystalline basement, belongs to the same stratigraphic range.

The acquired age data support a contemporaneous origin of the Permian sedimentary basin with the volcanic event and the dyke formation in the crystalline basement. Based on the whole-rock geochemical composition, the studied volcanic rocks correspond to weakly alkaline suite (trachyandesite to rhyolite/dacite). They exhibit light rare earth elements enrichment (La_N/Yb_N = 9.5–17.7) and small negative or absent Eu anomalies (Eu/Eu* = 0.95 and 1.05 for the Permian volcanites and 0.73 for the volcanic dyke). Characteristic of these volcanites is the enrichment in Cs, Rb, Th, U, K and Pb and the depletion in Nb, Ta, Sr and Ti if compared with average primitive mantle composition. All the studied volcanic rocks have low Nb/Ta (0.29–0.38) and Nb/U (4.07 to 5.87) ratios, implying a crustal magmatic source. Based on the incompatible trace elements Ta, Th and Yb, the Permian volcanics as well as the volcanic dyke cutting the crystalline basement fall close to the boundary between active continental margin and the within-plate fields.

The 358 ± 4 Ma magmatic zircon concordia age confirmed the Early Mississippian (Tournaisian) intrusion of the metatonalites in the Volchovo Valley, later blastomylonitized and covered by Permian siliciclastics.

Keywords: magmatic zircon dating, geochemistry, Permian volcanism, Central Western Carpathians
Received: 5 December, 2015; accepted: 2 August, 2016; handling editor: M. Kohút

1. Introduction

The Western Carpathians are the east–west trending range of the European Alpides, linked to the Eastern Alps in the west and to the Eastern Carpathians in the east, consisting of several northward-stacking thick-skinned crustal-scale superunits and several cover nappe systems. They have been traditionally divided into the outer and inner structural zones (Andrusov 1968; Mahel' 1986; Biely et al. 1996a, b; Plašienka et al. 1997 and references therein). The main differences between the outer and inner zones are the timing of the Alpine nappe emplacement and the intensity of related deformational and metamorphic events. Fragments of the medium- to high-grade crystalline complexes and their late Paleozoic and Mesozoic cover are inferred as integral parts of the following tectonic units: Tatricum, Northern and Southern Veporicum, Zemplinicum, Hronicum and Northern and Southern Gemericum, from the northern margin towards the southern parts of the Inner Western Carpathians. The same is the vertical sequence of the Alpine nappe units from the bottom to the top.

Late Palaeozoic volcanites of the Northern Veporicum (NV) are associated either with Permian siliciclastic sediments (Ľubietová Group, Vozárová 1979) or form bodies together with micrgranites and granites in the underlying crystalline complexes (Zoubek 1957; Bezák et al. 2008). The stratigraphic evidence of the Permian age of the sedimentary rocks is based only on the observation that they are overlain by the Lower Triassic sediments. Therefore, dating of associated volcanites will help to verify their Permian age. Two zircon samples from the Harnobis volcanogenic horizon (Brusno Fm.) and one from a volcanic dyke within the Ľubietová Crystalline Complex were analysed.

The volcano-metasedimentary complex from Volchovo Valley near Polomka was originally considered to be Permian (Klinec and Vozár 1971; Klinec 1976) as supported by the poor palynomorph assemblages that were classified by Planderová and Miko (1977) as Permian. To verify the age of underlying metatonalites in the Upper Hron Valley, an additional sample from Volchovo Valley was analysed. The tonalitic blastomylonite from their footwall was ascribed either to the Permian cover or to the crystalline basement.

The main goal of this study was, using the SHRIMP U–Pb dating on zircon, to establish the absolute age of the Harnobis Volcanogenic Horizon and its stratigraphic position in the whole Permian System. An additional objective was dating the metatonalite tectonic slice overthrusting the northveporic micaschists in the Upper Hron River Valley.

2. Geological setting

2.1. Western Carpathians

The north-vergent nappe system that affected Palaeozoic to Tertiary rocks is the principal feature of the Western Carpathians tectonic structure. The Western Carpathians are divided into two main tectonic zones with a contrasting history and a specific structural character: the Inner Western Carpathians (IWC) in the south and the Outer Western Carpathians (OWC) in the north. A narrow Klippen Belt rims the contact of the Inner and Outer Western Carpathians, usually considered as a part of the latter (Biely et al. 1996a and references therein). The age of the main Alpine events and the intensity of deformation and metamorphic grade are the main differences between the individual structural zones. These are: i) Internal Zone (IWC) that consists of the rocks affected by the Late Jurassic HP/LT (subduction) event and Early/Middle Cretaceous collision, followed by nappe stacking. This pre-Late Cretaceous nappe system includes the crystalline massifs with their Late Paleozoic Mesozoic cover sequences. ii) External zone (OWC) that underwent Late Cretaceous/Early Palaeocene to the Oligocene/Early Miocene subduction/accretion and collision events (Biely et al. 1996a; Plašienka 1998 and references therein).

Characteristic features of the Inner Western Carpathian units are: abundant pre-Late Carboniferous crystalline rocks (ortho- and paragneisses, amphibolites, migmatites, mica schists and granitoids), Late Paleozoic coarse-grained continental sediments and volcanites, carbonate Mesozoic complexes, and post-nappe Upper Cretaceous to Neogene cover. Specific members are tectonic outliers of the low-grade metamorphic rocks of Silurian–Devonian age (Bajaník et al. 1979; Miko 1981). Their thrusting over the crystalline basement was the result of Late Variscan collision, because both are covered by Permian post-collisional rock sequence (Vozárová and Vozár 1988; Putiš 1991; Biely et al. 1996b).

The pre-Late Cretaceous structure is formed by two types of nappe units. The first consists of pre-Late Carboniferous basement overlain by Late Palaeozoic and Mesozoic envelope sequences. This group of nappes comprises the Tatricum, Veporicum (including Zemplinicum) and the Gemericum megaunits. The second type is represented by rootless nappes composed dominantly of Mesozoic, and in some cases of Late Palaeozoic, rocks. This group consists of the Krížna nappe (Fatricum Unit), Choč and Šturec nappes (Hronicum Unit) and the structurally highest nappes, the Silicicum, Turnaicum and Meliaticum units (for further information see Andrusov 1968; Maheľ and Buday eds 1968; Kozur and Mock 1973, 1995, 1997; Mišík et al.1985; Maheľ 1986; Biely et al. 1996a, b; Plašienka 1998 and references therein).

2.2. Characteristics of the Veporicum Megaunit

The Veporicum Megaunit was divided into two subunits: a) the Northern Veporicum with Permian red-beds and the "Carpathian Keuper" in the Triassic sequence, and the Jurassic–Early Cretaceous succession; b) the Southern Veporicum with continental Upper Pennsylvanian–Permian sediments, Middle Triassic platform carbonates and Upper Triassic carbonates and black shales instead of the "Carpathian Keuper" facies (Vozárová and Vozár 1988; Biely et al. 1996a; Plašienka et al. 1997).

The tectonic contact between the Southern and Northern Veporicum units is represented by the Pohorelá Line in present geological maps. The Northern Veporicum is considered to be the root zone of the Krížna nappe s. l. on the Fatricum Unit (Jaroš 1969; Andrusov et al. 1973; Biely et al. 1996a).

Lithostratigraphy of the Northern Veporicum Permian sequence. Permian basins of the Northern Veporicum Zone were filled with continental volcano-sedimentary formations. They covered the underlying crystalline rock complexes with distinct unconformity and are separated by a hiatus and unconformity from the overlying Lower Triassic sediments.

The Permian sequence, as the basal part of the northveporic crystalline basement cover, is represented by the Ľubietová Group (Vozárová 1979) that comprises the lower Brusno and the upper Predajná formations (BF and PF, respectively). The consequence of northwestward overthrusting of the northveporic crystalline complexes was a tectonic reduction of the BF basal part (see tectonic profiles in Vozár 1965). The autochthonous position of the Ľubietová Group in relation to the northveporic crystalline basement has been proven by the provenance of clastic sediments in both formations (Vozárová 1979).

Principal lithostratigraphic characteristics of the BF are: i) dominant arkosic sediments and ii) presence of the Harnobis Volcanogenic Horizon (HVH) in the middle part. Generally, the BF consists of multiple repeating of tabular bodies of sandstones and fine-grained sandy conglomerates of variable thickness. Erosive contacts are frequent. The colour of sediments is uniform, mostly light-grey and light greenish-grey. The variable thickness (150–700 m) of the BF was controlled mainly by syn-sedimentary tectonics, and then by tectonic reduction due to the Alpine nappe stacking and overthrusting. Sediments of the BF indicate an environment of low-sinuosity rivers characterised by network of braided distributary channels transporting abundant coarse-sandy material. Frequent washouts, erosive channels as well as poorly preserved fine-grained sediments are taken as an evidence of quick and chaotic changes of braided channels with autocyclic erosive processes.

The HVH horizon is 150–200 m thick. It consists mostly of dacite–andesite effusions associated with prevalent pyroclastic tuffs (ignimbrites). Volcanic effusions are generally less frequent; some occur in the form of horizontal subsurface dykes. Volcanites are green-grey, green, and sometimes violet-grey.

The BF is unconformably overlain by the coarse-grained sediments of the PF. This unit reflects a conspicuous change in both the drainage system and the source area reflected in different petrographic composition of the clastic sediments. The PF is composed of variegated conglomerates, sandstones and shales with a thickness about 300–400 m. The principal characteristics of the PF are: i) megacyclic arrangement of the whole sequence; ii) conspicuous vertical and lateral changes in lithofacies; iii) polymictic clastic material; iv) absence of syn-sedimentary volcanic activity and the presence of reworked fragments derived from the underlying HVH volcanites.

Ilavský et al. (1994) presented a biostratigraphic evidence for the Permian age of both formations, based on pollen and spores determined by Planderová, from the borehole Lu-3 near Ľubietová Village.

Metatonalites of Volchovo Valley. Klinec (1976) correlated this rock complex with the Permian volcanic sequence of the Northern Veporicum, although this remains problematic. The detailed geological map of Putiš (1991) documented that a Permian volcano-sedimentary complex covers the tectonic slices of the Sihla southveporic granite–tonalite pluton, tectonically overlying northveporic micaschist basement. Therefore, Putiš (1991) correlated the Permian–Triassic cover of tonalites between Polomka and Heľpa with the southveporic Foederata Group sequence. Similar northveporic basement micaschists were correlated either with the low-grade metamorphic Early Paleozoic succession (Miko 1981; Korikovskij and Miko 1992) or they were considered as retrogressed paragneisses (Kubíny 1959; Zoubek 1957; Maheľ et al. 1964; Kamenický 1968; Maheľ and Buday eds 1968). U–Pb zircon dating of the northveporic acid to intermediate volcanic and subvolcanic rocks in Ľubietová and Bacúch (Jánov Grúň) areas determined a Permian age of this volcano-sedimentary complex (258 ± 2, 263 ± 3, 272 ± 10 Ma; Kotov et al. 1996). These rock complexes show low-temperature and medium-pressure metamorphic overprint (Korikovsky et al. 1997) of the Late Cretaceous age according to "phengitic" white mica $^{40}Ar/^{39}Ar$ dating (78 ± 1.3 Ma and 84 ± 3 Ma Ma, respectively; Kohút et al. 2000; Putiš et al. 2009a). No remnants of Devonian low-grade metaigneous rocks were confirmed from the north-veporic area by the newer SHRIMP U–Pb zircon dating (older zircon ages 525–480 Ma and younger 480–440 Ma, Putiš et al. 2008, 2009b).

3. Analytical methods

Zircons have been separated from rocks by standard grinding, heavy liquid (bromoform) and magnetic separation procedures. The selected crystals were mounted in the epoxy resin with chips of the TEMORA (Middledale Gabbroic Diorite, New South Wales, Australia; Black et al. 2003) and 91500 (Wiedenbeck et al. 1995) reference zircons. The zircons were imaged by optical microscopy, back-scattered electrons (BSE) and cathodoluminescence (CL), in order to guide the analytical spots positioning. *In situ* U–Pb analyses were performed on a SHRIMP-II in the Centre of Isotopic Research (CIR) at VSEGEI, St.-Petersburg, Russia, applying a secondary electron multiplier in peak-jumping mode following the procedure described by Williams (1998) and Larionov et al. (2004). Each analysis consisted of five scans through the 196–254 AMU mass range; analytical pit diameter was ~25 µm, with primary beam intensity of *c.* 6 nA. The primary beam size allowed analysis of *c.* 27 × 20 µm area. The 80 µm wide ion source slit, in combination with a 100 µm multiplier slit, allowed mass-resolution M/ΔM ≥ 5000 (1% valley); hence, all the possible isobaric interferences were resolved. The following ion species were measured in the sequence: $^{196}(Zr_2O)$–^{204}Pb–background (*c.* 204 AMU)–^{206}Pb–^{207}Pb–^{208}Pb–^{238}U–^{248}ThO–^{254}UO. Four cycles for each analysis were acquired. Each fifth measurement was carried out on the TEMORA Pb/U standard (Black et al. 2003). The 91500 zircon (Wiedenbeck et al. 1995) was applied as "U-concentration" standard.

The data have been reduced in a manner similar to that described by Williams (1998, and references therein), using the SQUID Excel Macro of Ludwig (2005a). The Pb/U ratios have been normalized relative to the value of 0.0668 for the $^{206}Pb/^{238}U$ ratio of the TEMORA reference zircons, equivalent to the age of 416.75 Ma (Black et al. 2003). Common lead was corrected using the measured ratio of $^{204}Pb/^{206}Pb$ (Stacey and Kramers 1975). Age calculations and plotting was done with ISOPLOT/EX (Ludwig 2005b). Uncertainties given for individual analyses (ratios and ages) are at the one σ

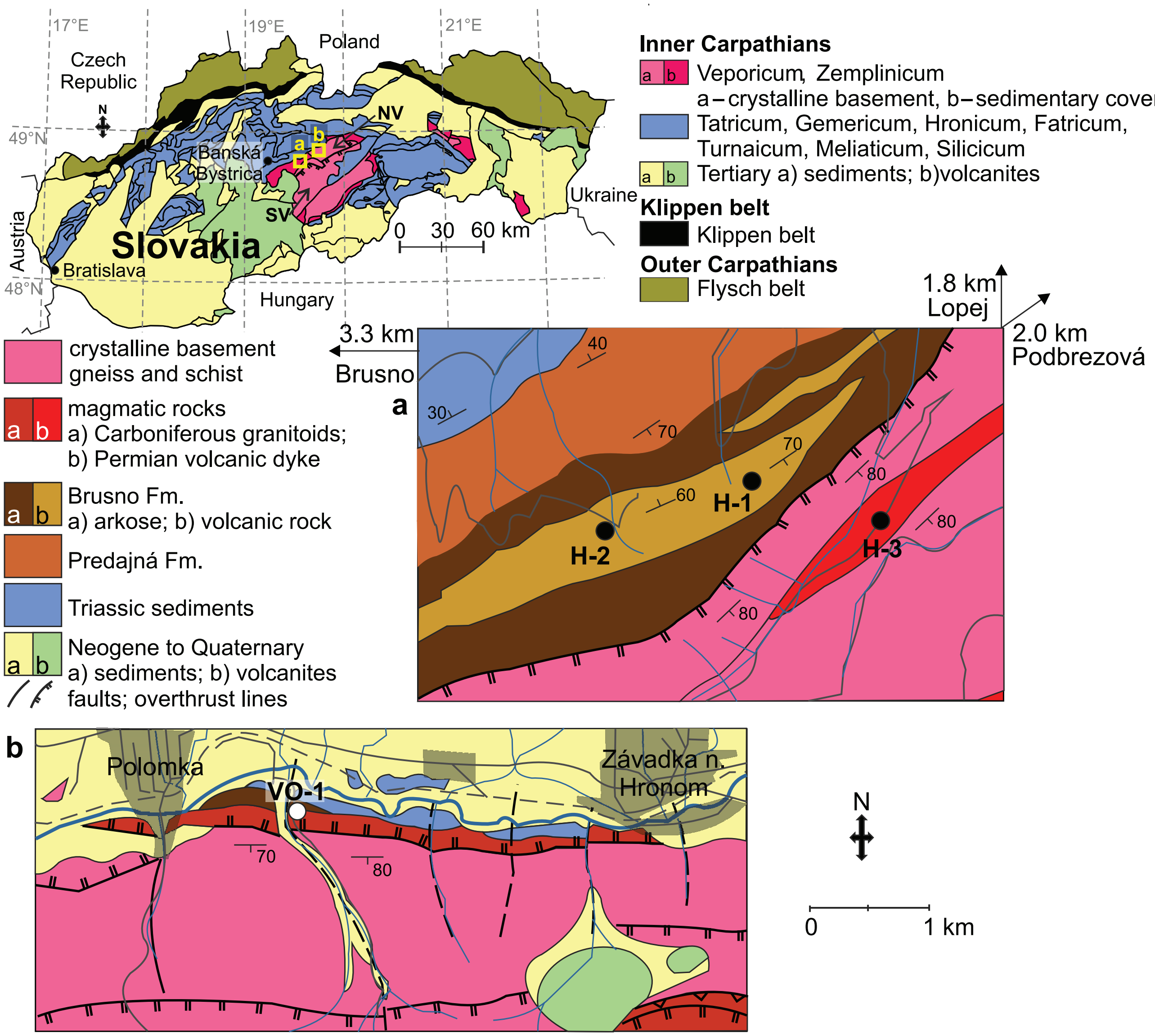

Fig. 1 Simplified geological sketch map of the Western Carpathians with the indication of the Northern and Southern Veporicum units (modified after Biely et al. 1996b). NV – Northern Veporicum; SV – Southern Veporicum. **a** – Schematic geological map of the NE part of the Northern Veporicum Permian sequence showing sample locations of the studied volcanic rocks (modified from Polák ed 2003). **b** – Schematic map of the studied area in the Volchovo Valley (modified from the Digital Geological Map of Slovakia 1 : 50 000 and Putiš 1991).

level; however, the uncertainties in calculated concordia ages are reported at two σ levels.

All dated samples were analysed for whole-rock composition in ACME Laboratories Ltd., Vancouver, Canada (*http://www.acmelab.com*; codes: 4A & B – Whole-Rock Analysis Major and Trace Elements). Following a lithium metaborate/tetraborate fusion and dilute nitric digestion, major elements were analyzed by inductively coupled plasma optical spectrometry (ICP-OES) and trace elements (including rare earth elements, REE) by inductively coupled plasma mass spectrometry (ICP-MS). The precision was checked using geological standard materials and it is estimated to be ± 1 % (1σ) for major elements (except ± 3 % for P_2O_5), and ± 10 % for trace elements.

4. Sample characteristics

Two samples have been collected from the HVH volcanites for zircon dating (Fig. 1a). These are ***H-1***, located SE of the Nemecká Village, *c.* 350 m W of the Holý vrch e.p. (1090 m), 990 m a.s.l., GPS: N 48°47'060"; E 19°27'991" and ***H-2***, located SE of the Nemecká Village, on the western slopes of the Harnobis, 940 m a.s.l., *c.* 1.5 km W of the Holý vrch e.p. (1090 m), GPS: N 48°47'713"; E 19°27'660". For correlation serves sample ***H-3*** from a dacite dyke of the Ľubietová Zone crystalline basement. It was located in the Predajnianske Čelno Valley, Kelemen᾿s tunnel, 875 m a.s.l, GPS: N 48°46'564", E 19°29'039".

The last sample, ***VO-1***, comes from a narrow zone of metatonalites covered by inferred Permian metaclastics south of the Hron River between Polomka and Heľpa villages (Fig. 1b). It was collected from the mouth of the Volchovo Valley, south of the Polomka Village, 627 m a.s.l., GPS: N 48°45'802", E 19°52'192".

5. Petrographic features and chemical composition

5.1. Petrography

The *H-1* and *H-2* volcanic rocks display an ignimbritic structure and texture variably consisting of flattened pumice, recrystallized fragments of glass, felsitic rock fragments and various broken crystals. The rocks are irregularly foliated, showing a recrystallization of the originally glassy groundmass. Broken and corroded quartz, plagioclase and highly altered biotite are dominant. Biotite crystals show marked chloritization and hematitisation, associated with patches of Fe-oxy-hydroxide. Locally, relics of mafic crystals are present, totally altered to aggregate of chlorite, epidote and titanite that may indicate amphibole as the possible reaction precursor. The euhedral to anhedral plagioclases are broken and very often deformed along foliation planes, intensively altered to albite and replaced by secondary muscovite. Scarce K-feldspar phenocrysts are perthitic. Occasional calcite and epidote grains were identified among secondary minerals; zircon, apatite and allanite are the common accessories.

On the contrary, the sample *H-3* displays the volcanic, porphyritic or glomerophyric texture, with fine-grained, deformed and partly foliated groundmass. Quartz and plagioclase are dominant phenocrysts, associated with the relics of highly altered biotite and subordinate K-feldspar. The orthoclase phenocrysts include exsolved lamellae of albitic feldspar. All crystals in this volcanic dyke show magmatic corrosion features, i.e. embayed quartz and relics of sieve texture in plagioclase. Plagioclase grains have albitic rims enclosing the saussuritized primary An-rich cores. Individual quartz and feldspars crystals are rounded by resorption. The sieve microtexture of plagioclases is usually interpreted as resulting from magma mixing, but it may also originate by rapid decompression, when the heat loss is minor due to a high ascent rate (Nelson and Montana 1992 and references therein).

Generally, the groundmass of all three samples (*H-1*, *H-2* and *H-3*) is only slightly foliated and deformed. Recrystallization is documented by the newly-formed aggregates of muscovite, quartz and, less frequently, chlorite, epidote and calcite. Secondary alteration is documented by the complete alteration of plagioclase to albite or saussurite mixture and total chloritization and/or baueritization of biotite. The amphibole phantom phenocrysts were replaced by a mixture of epidote, chlorite, and titanite, occasionally with apatite and allanite inclusions.

The sample *VO-1* displays a lepidogranoblastic texture, whereby the high degree of its recrystallization correlates with a distinct foliation and crenulation cleavage. Blastomylonitic foliation is marked by alternating bands of different mineralogical composition (rich in quartz–albite and mica). The cleavage domains are marked by concentrations of fine-grained white mica aggregates and/or opaque mineral substance, identified as fine crystals of magnetite/Ti-magnetite. Zircon, apatite, tourmaline and rutile were detected among accessory minerals. The newly-formed white mica from granitoid blastomylonites and of the Permian cover metaclastics was dated at 84 ± 3 Ma by $^{40}Ar/^{39}Ar$ method (Putiš et al. 2009a).

5.2. Geochemistry

All studied rocks underwent a significant degree of metasomatism and secondary alteration (Tab. 1). This is reflected especially by LOI values, which vary from 2.0 to 2.5 wt. %. Therefore, all major-element analyses were recalculated on a volatile-free basis. The major oxides show 1.3–1.5 wt. % MgO and 67.7–70.5 wt. % SiO_2. As the sample *VO-1* represents a strongly blastomylonitized tonalite, its geochemical characteristics were plotted in diagrams together with the volcanic rocks.

The studied volcanites belong to the peraluminous group, with ratios of A/NK = 1.37–1.51 and A/CNK = 1.11–1.13 (samples *H-1, 2, 3*) and 1.77 and 1.68 respectively *(VO-1)*. Consequently, the classification of studied rocks as well as the discussion of whole-rock geochemistry mainly focuses on relatively immobile elements such as Ti, Th, U, Zr, Nb, Ta, Y and REE. In the Zr/TiO_2 vs. Nb/Y diagram (Winchester and Floyd 1977) the samples

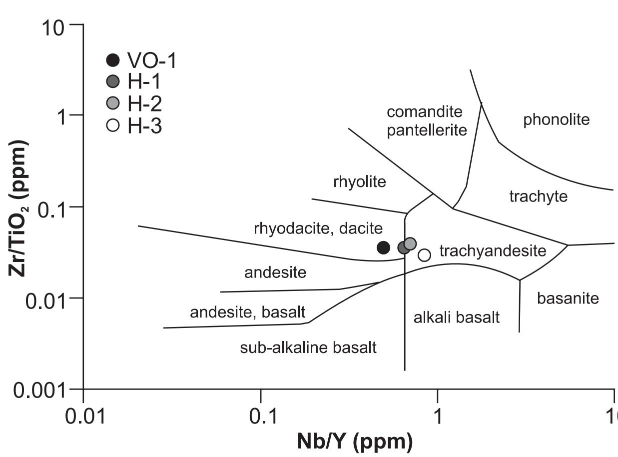

Fig. 2 Classification of the studied samples in Zr/TiO_2 vs. Nb/Y diagram (after Winchester and Floyd 1977).

Tab. 1 Major (wt. %) and trace-element (ppm) whole-rock analyses from the studied rocks

sample	**H-1**	**H-2**	**H-3**	**VO-1**
SiO_2	65.9	66.4	66.2	69.6
TiO_2	0.42	0.36	0.56	0.56
Al_2O_3	15.9	16.4	15.8	14.1
Fe_2O_3	3.99	3.39	3.93	5.25
MnO	0.06	0.07	0.05	0.03
MgO	1.46	1.27	1.47	1.29
CaO	2.04	1.51	1.39	0.22
Na_2O	4.32	5.34	5.21	1.73
K_2O	3.14	2.94	2.71	4.74
P_2O_5	0.15	0.15	0.14	0.12
Cr_2O_3	0.006	0.005	0.005	0.010
LOI	2.5	2.0	2.5	2.2
Total	99.83	99.83	99.96	99.85
Ba	594	429	354	813
Cs	10.0	7.8	5.4	39.7
Hf	3.9	3.8	4.4	5.8
Nb	7.5	6.4	10.6	9.4
Rb	97.7	92.7	95.3	224.4
Sr	342	378	163	49
Ta	0.8	0.7	0.8	0.7
Th	5.4	4.8	8.0	9.0
U	1.6	1.2	2.6	1.6
Zr	152	142	169	207
Y	11.6	9.2	12.5	19.1
La	22.2	22.1	27.5	26.0
Ce	41.6	41.1	52.5	58.6
Pr	5.06	4.97	6.48	6.31
Nd	18.5	19.1	23.4	23.0
Sm	3.31	3.05	4.10	4.00
Eu	0.92	0.93	0.87	0.93
Gd	2.62	2.38	3.19	3.59
Tb	0.38	0.33	0.46	0.58
Dy	2.08	1.74	2.26	3.36
Ho	0.39	0.31	0.43	0.67
Er	1.15	0.90	1.26	1.96
Tm	0.17	0.14	0.19	0.29
Yb	1.10	0.85	1.23	1.85
Lu	0.15	0.13	0.18	0.27
Pb	4.1	2.0	1.1	5.7
Eu/Eu*	0.95	1.05	0.73	0.75
A/NK	1.51	1.37	1.37	1.77
A/CNK	1.12	1.11	1.13	1.68

$Eu/Eu^* = Eu_N/(Sm_N \cdot Gd_N)^{(1/2)}$

H-1, *H-2* and *H-3* straddle the boundary of the alkaline series (the rhyolite/dacite and trachyandesite fields) while the sample *VO-1* is subalkaline (Fig. 2).

In the chondrite-normalized REE diagram these volcanic rocks (Fig. 3a) exhibit enrichment of light REE (LREE) and relative depletion of heavy REE (HREE) (La_N/Yb_N = 9.5–17.7) and small or no negative Eu anomalies (*H-1* and *H-2* = 0.95 and 1.05; *H-3* = 0.73; *VO-1* = 0.75). In the primitive-mantle normalized trace-element diagram (Fig. 3b) these rocks are enriched in Cs, Rb, Th, U, K and Pb (Pb with exception of the sample *H-3*) and depleted in Nb, Ta, Sr and Ti.

Generally, all the studied volcanic rocks have low Nb_N/Ta_N ratios (0.52–0.77). These values are near to the 0.71 crustal ratio (Rudnick and Fountain 1995), implying that crustal material has been involved in their magmatic source. Equally, the crustal involvement is indicated by low Nb/U ratios, ranging from 4.1 to 5.9 (9.7 value for continental crust according to Rudnick and Fountain 1995).

Gorton and Schandl (2000) proposed a series of geotectonic diagrams for acid and intermediate volcanic rocks based on concentrations of the incompatible trace elements Ta, Th and Yb. They also revised the Th/Yb vs. Ta/Yb diagram of Pearce (1983) and divided it into three tectonic fields: oceanic islands (OA), active continental margins (ACM) and within-plate volcanic zones (WPVZ). The HVH volcanites (samples *H-1*, *H-2*) as well as the volcanic dyke (*H-3*) straddle the boundary between the ACM and WPVZ volcanites (Fig. 4). They have relatively low Th/Ta values (6.8–6.9 and 10.0, respectively). Compared to the other samples, the *VO-1* blastomylonite reliably plots in the ACM field.

6. Zircon age data

The presence of the xenocrystic zircon is a common feature of all studied samples (Fig. 5). Most zircon xenocrysts occur as cores mantled by newly grown magmatic zircon rims but some are unmantled, subrounded or even euhedral grains. This indicates an incorporation into magma during the late-stage crystallization, with too little time for corrosion and overgrowths (Corfu et al. 2003). The xenocrystic zircon cores are distinguished from their rims by irregular surfaces, which truncate internal zoning and separate the subrounded or chaotically zoned cores from growth-zoned rims. The rims are darker than the cores, indicating U enrichment (Hanchar and Miller 1993; Poller et al. 2001) (Fig. 5).

Zircon dating from the samples *H-1* and *H-2* documents the Cisuralian (early Permian) age of the Harnobis volcanogenic horizon (Tabs 2–3) with concordia ages of 273 ± 6 Ma and 279 ± 4 Ma (Figs 6–7) respectively (Kungurian). The outermost zones of magmatic zircons yielded a concordia age of 244 ± 6 Ma (Fig. 6), which might reflect a reheating during the Alpine extension and possible Pb-loss. The concordia zircon age from the dyke of the Kelemen's tunnel area, sample *H-3*, confirmed the Kungurian age – 272 ± 4 Ma as well (Fig. 8). In all three samples xenocrystic cores were found within magmatic zircons yielding the following concordia ages: 352 ± 15 Ma, 458 ± 14 Ma, 501 ± 21 Ma, 655 ± 19 Ma, 659 ± 18 Ma,

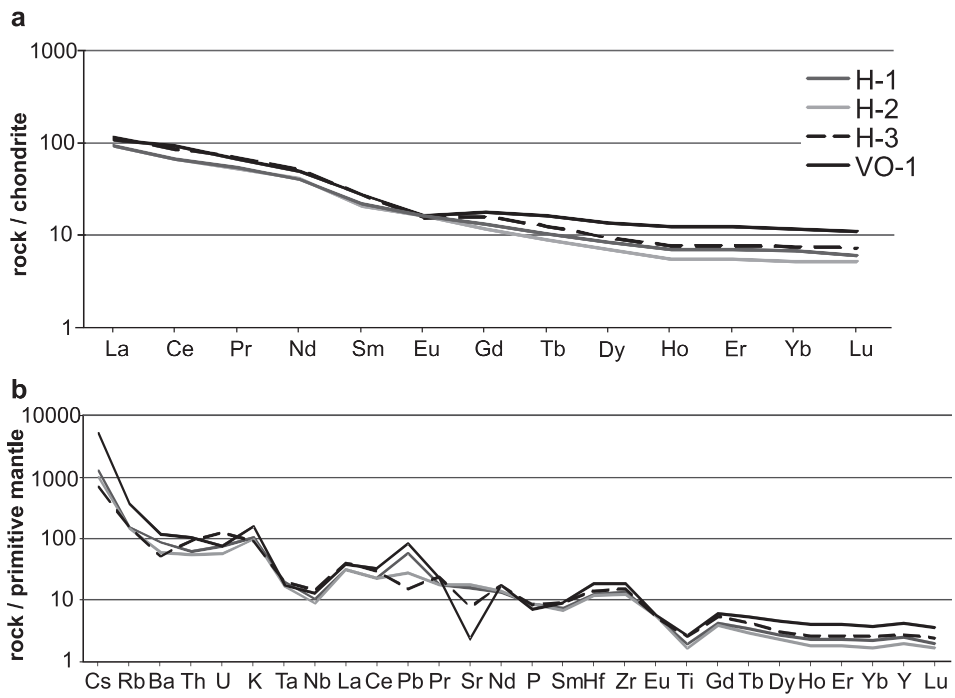

Fig. 3a – Chondrite-normalized REE patterns of the Harnobis Volcanogenic Horizon (HVH) volcanic rocks, metatonalite and the intra--crystalline dyke. Chondrite normalizing values are after McDonough and Sun (1995). **b** – Multi-elements variation diagram of the Northern Veporicum Permian volcanic rocks, metatonalite and the intra-crystalline dyke. Primitive mantle normalizing values are after Sun and McDonough (1989).

821 ± 34 Ma, 939 ± 25 Ma, 971 ± 26 Ma, as well as one Archean age of ~2.7 Ga (Tabs 2–4). These ages document the presence of multiple zircon core formation events and/or varying degrees of Pb loss.

The concordia age from the metatonalites of Volchovo Valley (sample *VO-1*) confirms the Early Mississippian (Tournaisian) age, 358 ± 4 Ma (Fig. 9). In addition xenocrystic cores were identified, yielding an Early Cambrian concordia age – 516.7 ± 8.6 Ma (Tab. 5). The Early Mississippian (Tournaisian) age of magmatic zircons from metatonalite slices at the mouth of the Volchovo Valley is compatible with zircon ages of the Vepor pluton granitic rocks, including the Sihla-type tonalites (350 ± 4.4 Ma – Kohút et al. 2008; 357 ± 2 Ma – Broska et al. 2013), as well as from the granitoid rocks of the Nizke Tatry Mts (356 ± 10 and 359 ± 6 Ma, respectively – Gaab et al. 2005).

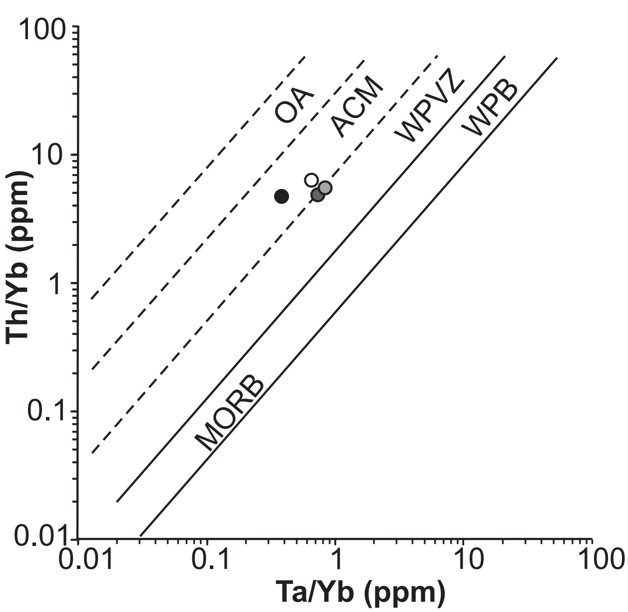

Fig. 4 Gorton and Shandl's (2000) geotectonic diagram Th/Yb vs. Ta/Yb (modified from Pearce 1983). Abbreviations: oceanic arcs (OA), active continental margins (ACM), within-plate volcanic zones (WPVZ), within-plate basalts (WPB) and MORB (mid-ocean ridge basalts).

7. Discussion

A Permian age of the HVH volcanites was presumed based on their (i) occurrence inside of the coarse-grained arkosic continental deposits, and (ii) superposition between the Ľubietová Zone crystalline basement and the quartzitic Lower Triassic sediments (Zoubek 1936, 1957; Maheľ et al. 1964, Kamenický 1977; Vozár 1979; Vozárová 1979). The newly obtained *in situ* U–Pb magmatic zircon ages, on average *c.* 275 Ma, enable us to assign the HVH volcanic rocks to the uppermost Cisuralian, accurately in the Kungurian (according to the International Stratigraphic Chart 2014). The similar 272 ± 4 Ma U–Pb zircon age, obtained from the volcanic dyke cutting the crystalline basement, belongs also to the Kungurian (Fig. 10).

These ages agree well with zircon and monazite ages of the Permian volcanic horizons from the Southern and Northern Gemericum Units, in which the Kungurian volcanic event was dominant (CHIME monazite age 278 ± 10 Ma – Rojkovič and Konečný 2005; monazite age 276 ± 25

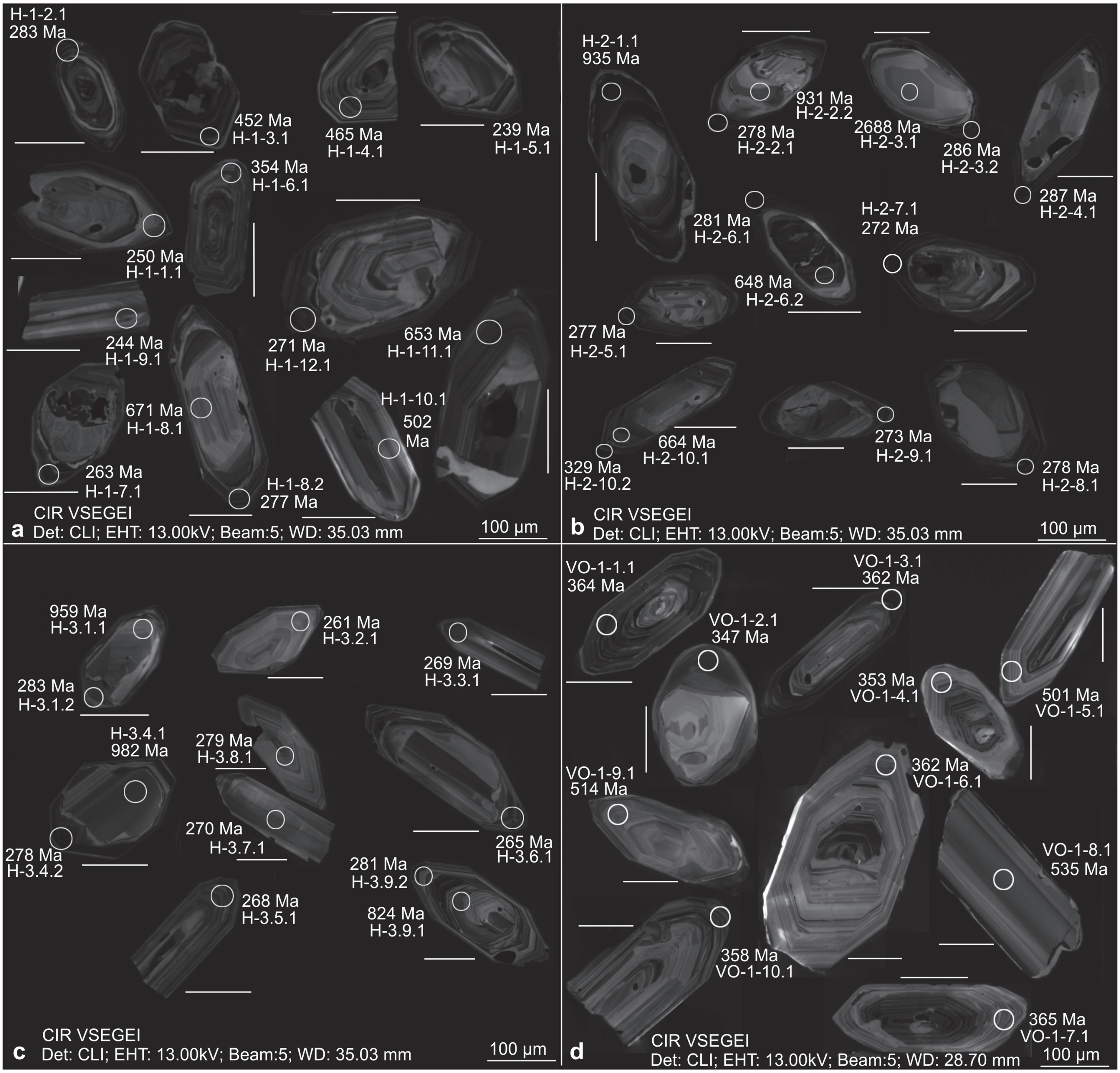

Fig. 5 Selected cathodoluminescence images of magmatic zircon with $^{206}Pb/^{238}U$ ages (Ma): **a** – *H-1*; **b** – *H-2*; **c** – *H-3*; **d** – *VO-1*.

Ma – Vozárová et al. 2008, U–Pb SHRIMP zircon age – 275±3 Ma Vozárová et al. 2009a, U–Pb SHRIMP zircon ages of 272±7 Ma and 275±4 Ma – Vozárová et al. 2012). The youngest Permian volcanic ages have been proven by both Re–Os molybdenite geochronology (257±3 and 256±4 Ma – Kohút et al. 2013), and by U–Pb zircon dating (251±4 Ma – Vozárová et al. 2015) from the Northern Gemericum Unit, as well as from the Bôrka Nappe of the Meliaticum Unit (266±2 Ma – Vozárová et al. 2012).

Correspondingly, rhyodacites and associated ignimbrites are widespread at the top of the Cisuralian succession in the Eastern and Southern Alps and are correlated with the Bolzano Volcanic Complex (Cortesogno et al. 1998; Klötzli et al. 2003; McCann et al. 2008; Cassinis et al. 2012 and references therein). Similarly, the Cisuralian volcanism was also documented in the Mecsek and Apuseni Mts. (Balogh and Kovách 1973; Bleahu et al. 1981; Stan 1984; Seghedi et al. 2001; Nicolae et al. 2014), in the Bucovinian-Getic and Danubian nappe systems within the Eastern and Southern Carpathians (Stan 1987; Kräutner 1997), as well as in the Serbian Carpatho-Balkanides (Krstić and Karamata 1992) and Bulgarian Balkanides (Cortesogno et al. 2004). In all these areas all the Cisuralian volcanic activity was strictly connected with extensional tectonic events.

Generally, the Late Paleozoic–Early Triassic time was marked by the transition from the Variscan orogeny to the Alpine tectono-sedimentary cycle, which was induced

Tab. 2 SHRIMP zircon age data from the sample H-1

Spot	$^{206}Pb_c$ (%)	U (ppm)	Th (ppm)	$^{232}Th/^{238}U$	$^{206}Pb^*$ (ppm)	(1) Age $^{206}Pb/^{238}U$	(1) Age $^{207}Pb/^{206}Pb$	Disc (%)	Total $^{238}U/^{206}Pb$	(%) ±	Total $^{207}Pb/^{206}Pb$	(%) ±	(1) $^{238}U/^{206}Pb^*$	(%) ±	(1) $^{207}Pb^*/^{206}Pb^*$	(%) ±	(1) $^{207}Pb^*/^{235}U$	(%) ±	(1) $^{206}Pb^*/^{238}U$	(%) ±	corr
H-1– 5.1	0.20	602	235	0.40	19.6	239±5.3	276±66	15	26.44	2.3	0.05338	1.5	26.50	2.3	0.0518	2.9	0.2694	3.7	0.0377	2.3	0.618
H-1– 9.1	0.25	371	93	0.26	12.3	244±5.5	258±64	5	25.82	2.3	0.05340	1.9	25.88	2.3	0.0514	2.8	0.2737	3.6	0.0386	2.3	0.635
H-1– 1.1	0.62	531	104	0.20	18.1	250±5.6	278±93	11	25.16	2.3	0.05676	1.5	25.32	2.3	0.0518	4.1	0.2820	4.7	0.0395	2.3	0.492
H-1– 7.1	0.05	1169	218	0.19	41.9	263±5.8	256±31	–3	23.97	2.2	0.05173	1.1	23.98	2.2	0.0514	1.3	0.2953	2.6	0.0417	2.2	0.859
H-1–12.1	0.00	927	238	0.27	34.1	271±6.0	277±30	2	23.32	2.3	0.05164	1.3	23.31	2.3	0.0518	1.3	0.3063	2.6	0.0429	2.3	0.867
H-1– 8.2	0.50	987	241	0.25	37.5	277±6.1	251±69	–9	22.64	2.2	0.05528	1.2	22.75	2.2	0.0512	3.0	0.3100	3.7	0.0439	2.2	0.603
H-1– 2.1	0.20	776	225	0.30	30.0	283±6.2	281±54	0	22.27	2.3	0.05351	1.5	22.32	2.3	0.0519	2.4	0.3210	3.3	0.0448	2.3	0.687
H-1– 6.1	0.07	549	438	0.82	26.6	354±7.8	326±39	–8	17.72	2.3	0.05347	1.4	17.73	2.3	0.0529	1.7	0.4110	2.8	0.0564	2.3	0.799
H-1– 3.1	1.00	650	122	0.19	40.9	452±9.9	498±62	10	13.64	2.3	0.06528	1.0	13.77	2.3	0.0572	2.8	0.5720	3.6	0.0726	2.3	0.627
H-1– 4.1	0.11	325	254	0.81	20.9	465±10	426±47	–8	13.36	2.3	0.05622	1.5	13.37	2.3	0.0553	2.1	0.5710	3.1	0.0748	2.3	0.734
H-1–10.1	0.06	321	207	0.67	22.4	502±11	485±34	–3	12.33	2.3	0.05730	1.5	12.34	2.3	0.0568	1.5	0.6350	2.7	0.0810	2.3	0.827
H-1–11.1	0.04	504	48	0.10	46.2	653±14	641±24	–2	9.37	2.2	0.06140	1.0	9.38	2.2	0.0610	1.1	0.8970	2.5	0.1066	2.2	0.899
H-1– 8.1	0.02	138	71	0.53	13.0	671±15	676±41	1	9.11	2.3	0.06230	1.9	9.11	2.3	0.0621	1.9	0.9390	3.0	0.1098	2.3	0.771

Disc = discordant; Errors are 1 sigma;
(1) Common Pb corrected using measured ^{204}Pb; Pb_c and Pb* indicate the common and radiogenic portions, respectively;
Error in Standard calibration was 0.71 % (not included in above errors but required when comparing data from different mounts).

Tab. 3 SHRIMP zircon age data from the sample H-2

Spot	$^{206}Pb_c$ (%)	U (ppm)	Th (ppm)	$^{232}Th/^{238}U$	$^{206}Pb^*$ (ppm)	(1) Age $^{206}Pb/^{238}U$	(1) Age $^{207}Pb/^{206}Pb$	Disc (%)	Total $^{238}U/^{206}Pb$	(%) ±	Total $^{207}Pb/^{206}Pb$	(%) ±	(1) $^{238}U/^{206}Pb^*$	(%) ±	(1) $^{207}Pb^*/^{206}Pb^*$	(%) ±	(1) $^{207}Pb^*/^{235}U$	(%) ±	(1) $^{206}Pb^*/^{238}U$	(%) ±	corr
H-2– 7.1	0.16	1860	605	0.34	68.9	272±6.1	281±56	3	23.20	2.3	0.0532	1.7	23.24	2.3	0.0519	2.4	0.308	3.3	0.0430	2.3	0.683
H-2– 9.1	0.68	1312	431	0.34	49.0	273±6.2	330±110	21	22.98	2.3	0.0585	2.0	23.14	2.3	0.0530	4.8	0.316	5.3	0.0432	2.3	0.439
H-2– 5.1	0.26	1662	377	0.23	62.9	277±6.3	291±77	5	22.68	2.3	0.0542	1.7	22.74	2.3	0.0521	3.4	0.316	4.1	0.0440	2.3	0.564
H-2– 8.1	0.42	2201	501	0.23	83.6	278±6.2	280±64	1	22.63	2.3	0.0552	1.5	22.72	2.3	0.0519	2.8	0.315	3.6	0.0440	2.3	0.629
H-2– 2.1	0.13	1951	489	0.26	73.9	278±6.2	279±52	0	22.68	2.3	0.0529	1.6	22.71	2.3	0.0519	2.3	0.315	3.2	0.0440	2.3	0.706
H-2– 6.1	0.26	2504	1294	0.53	96.2	281±6.3	319±66	13	22.36	2.3	0.0549	1.5	22.42	2.3	0.0528	2.9	0.324	3.7	0.0446	2.3	0.615
H-2– 3.2	0.24	1420	258	0.19	55.6	286±6.5	330±73	15	21.96	2.3	0.0550	1.8	22.01	2.3	0.0530	3.2	0.332	4.0	0.0454	2.3	0.584
H-2– 4.1	0.54	2341	1099	0.48	92.2	287±6.4	331±74	15	21.82	2.3	0.0574	1.4	21.94	2.3	0.0530	3.3	0.333	4.0	0.0456	2.3	0.572
H-2–10.2	0.38	919	202	0.23	41.5	329±7.6	347±110	6	19.05	2.3	0.0565	2.4	19.12	2.4	0.0534	4.8	0.385	5.4	0.0523	2.4	0.440
H-2– 6.2	0.10	972	88	0.09	88.3	648±14	668±34	3	9.45	2.3	0.0627	1.4	9.46	2.3	0.0618	1.6	0.901	2.8	0.1057	2.3	0.822
H-2–10.1	0.20	568	187	0.34	53.1	664±15	620±48	–7	9.20	2.3	0.0621	1.7	9.22	2.3	0.0604	2.2	0.904	3.2	0.1085	2.3	0.720
H-2– 2.2	0.62	96	73	0.79	12.9	931±25	962±110	3	6.39	2.8	0.0764	3.1	6.43	2.8	0.0712	5.4	1.525	6.1	0.1554	2.8	0.465
H-2– 1.1	0.07	1351	43	0.03	181.0	935±20	949±20	1	6.40	2.3	0.0713	0.9	6.41	2.3	0.0707	1.0	1.522	2.5	0.1561	2.3	0.914
H-2– 3.1	0.08	94	166	1.82	41.8	2688±56	2683±21	0	1.93	2.6	0.1840	1.3	1.932	2.6	0.1833	1.3	13.08	2.9	0.5170	2.6	0.894

Errors are 1 sigma; (1) Common Pb corrected using measured ^{204}Pb; Pb_c and Pb* indicate the common and radiogenic portions, respectively;
Error in Standard calibration was 0.71 % (not included in above errors but required when comparing data from different mounts).

Tab. 4 SHRIMP zircon age data from the sample H-3

Spot	$^{206}Pb_c$ (%)	U (ppm)	Th (ppm)	$^{232}Th/^{238}U$	$^{206}Pb^*$ (ppm)	(1) Age $^{206}Pb/^{238}U$	(1) Age $^{207}Pb/^{206}Pb$	Disc (%)	Total $^{238}U/^{206}Pb$	(%) ±	Total $^{207}Pb/^{206}Pb$	(%) ±	(1) $^{238}U/^{206}Pb^*$	(%) ±	(1) $^{207}Pb^*/^{206}Pb^*$	(%) ±	(1) $^{207}Pb^*/^{235}U$	(%) ±	(1) $^{206}Pb^*/^{238}U$	(%) ±	corr
H-3–2.1	0.00	187	111	0.62	6.6	261±6.5	231±78	–11	24.23	2.5	0.0499	3.0	24.21	2.5	0.0508	3.4	0.2890	4.2	0.0413	2.5	0.599
H-3–6.1	0.12	614	185	0.31	22.2	265±6.2	245±40	–8	23.76	2.4	0.0521	1.4	23.79	2.4	0.0511	1.7	0.2961	3.0	0.0420	2.4	0.812
H-3–5.1	0.00	567	201	0.37	20.7	268±6.3	257±34	–4	23.58	2.4	0.0514	1.5	23.58	2.4	0.0514	1.5	0.3002	2.8	0.0424	2.4	0.854
H-3–3.1	0.00	521	222	0.44	19.1	269±6.4	309±43	15	23.48	2.4	0.0521	1.8	23.46	2.4	0.0525	1.9	0.3087	3.1	0.0426	2.4	0.790
H-3–7.1	0.00	238	97	0.42	8.8	270±6.6	275±60	2	23.36	2.5	0.0518	2.6	23.36	2.5	0.0518	2.6	0.3060	3.6	0.0428	2.5	0.689
H-3–4.2	0.27	1298	19	0.02	49.3	278±6.5	268±36	–3	22.64	2.4	0.0538	0.9	22.70	2.4	0.0516	1.6	0.3134	2.9	0.0440	2.4	0.834
H-3–8.1	0.00	286	209	0.75	10.9	279±6.7	212±55	–24	22.58	2.5	0.0504	2.4	22.58	2.5	0.0504	2.4	0.3080	3.4	0.0443	2.5	0.719
H-3–9.2	0.37	495	300	0.63	19.0	281±6.7	264±80	–6	22.33	2.4	0.0545	1.8	22.42	2.4	0.0515	3.5	0.3170	4.2	0.0446	2.4	0.573
H-3–1.2	0.53	422	72	0.18	16.3	283±6.7	247±78	–13	22.18	2.4	0.0554	1.7	22.30	2.4	0.0511	3.4	0.3160	4.2	0.0448	2.4	0.584
H-3–9.1	0.00	250	113	0.47	29.3	824±19	809±39	–2	7.34	2.4	0.0659	1.9	7.33	2.4	0.0661	1.9	1.2430	3.1	0.1363	2.4	0.792
H-3–1.1	0.47	89	34	0.39	12.3	959±22	988±63	3	6.20	2.5	0.0760	1.8	6.23	2.5	0.0721	3.1	1.5940	4.0	0.1604	2.5	0.628
H-3–4.1	0.13	245	311	1.31	34.6	982±22	971±24	–1	6.07	2.4	0.0725	1.0	6.08	2.4	0.0715	1.2	1.6210	2.7	0.1645	2.4	0.900

Errors are 1 sigma; (1) Common Pb corrected using measured ^{204}Pb; Pb_c and Pb* indicate the common and radiogenic portions, respectively;
Error in Standard calibration was 0.68 % (not included in above errors but required when comparing data from different mounts).

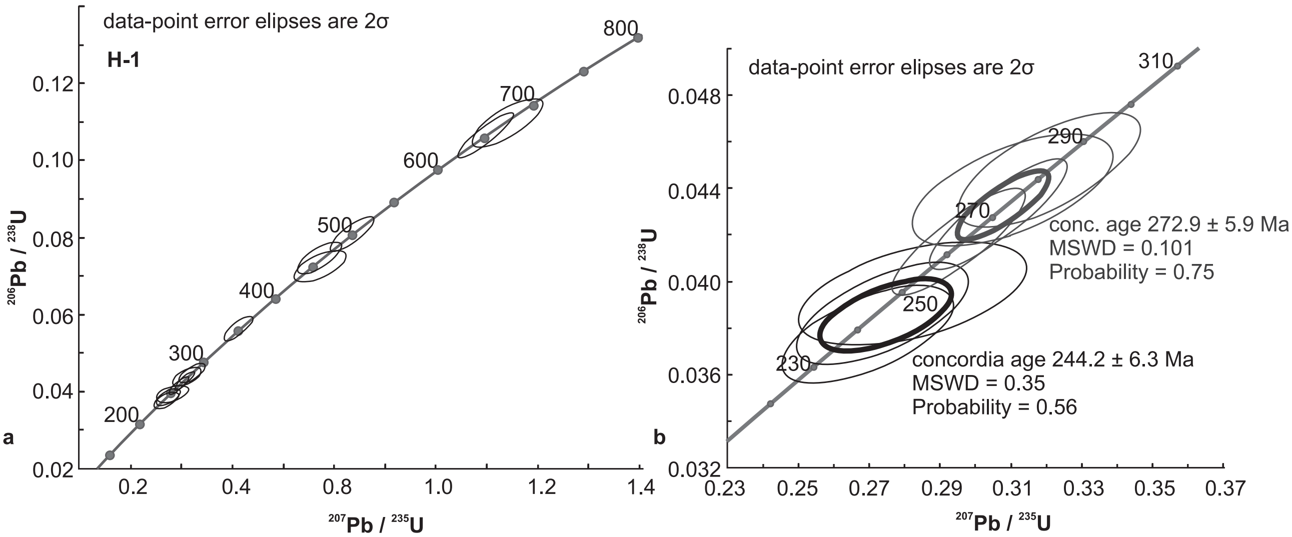

Fig. 6 Concordia plots showing the magmatic zircon ages from the sample *H-1,* and corresponding concordia ages: **a** – all data (n = 13); **b** – detail on Permian ages (black = 3, grey = 4).

Tab. 5 SHRIMP zircon age data from the sample VO-1

Spot	$^{206}Pb_c$ (%)	U (ppm)	Th (ppm)	$^{232}Th/^{238}U$	$^{206}Pb^*$ (ppm)	(1) Age $^{206}Pb/^{238}U$	(1) Age $^{207}Pb/^{206}Pb$	Disc (%)	(1) $^{238}U/^{206}Pb^*$	(%) ±	(1) $^{207}Pb^*/^{206}Pb^*$	(%) ±	(1) $^{207}Pb^*/^{235}U$	(%) ±	(1) $^{206}Pb^*/^{238}U$	(%) ±	corr
VO-1– 2.1	0.09	423	20	0.05	20.1	347.3 ± 5.2	374 ± 63	8	18.06	1.5	0.0541	2.8	0.413	3.2	0.05536	1.5	0.481
VO-1– 3.1	0.13	1156	16	0.01	57.5	362.1 ± 5.1	364 ± 28	1	17.31	1.4	0.0538	1.2	0.429	1.9	0.05777	1.4	0.754
VO-1– 4.1	0.16	278	109	0.40	13.5	352.7 ± 5.2	339 ± 62	–4	17.78	1.5	0.0532	2.7	0.413	3.1	0.05624	1.5	0.480
VO-1– 5.1	0.35	238	59	0.25	16.6	500.9 ± 7.2	515 ± 79	3	12.37	1.5	0.0576	3.6	0.642	3.9	0.08080	1.5	0.386
VO-1– 6.1	0.03	408	210	0.53	20.2	361.9 ± 5.1	290 ± 45	–20	17.32	1.4	0.0521	2.0	0.415	2.4	0.05774	1.4	0.589
VO-1– 7.1	0.06	339	230	0.70	17.0	364.5 ± 5.5	385 ± 48	6	17.19	1.6	0.0543	2.1	0.436	2.7	0.05818	1.6	0.589
VO-1– 8.1	0.23	295	226	0.79	22.0	535.2 ± 7.9	534 ± 50	0	11.55	1.5	0.0581	2.3	0.694	2.7	0.08660	1.5	0.561
VO-1– 9.1	0.38	209	54	0.27	14.9	513.5 ± 7.4	498 ± 71	–3	12.06	1.5	0.0572	3.2	0.654	3.6	0.08290	1.5	0.422
VO-1–10.1	0.32	553	222	0.41	27.2	357.8 ± 5.0	306 ± 61	–15	17.52	1.4	0.0525	2.7	0.413	3.0	0.05708	1.4	0.468

Errors are 1 sigma; (1) Common Pb corrected using measured ^{204}Pb; Pb_c and Pb* indicate the common and radiogenic portions, respectively; Error in Standard calibration was 0.53 % (not included in above errors but required when comparing data from different mounts).

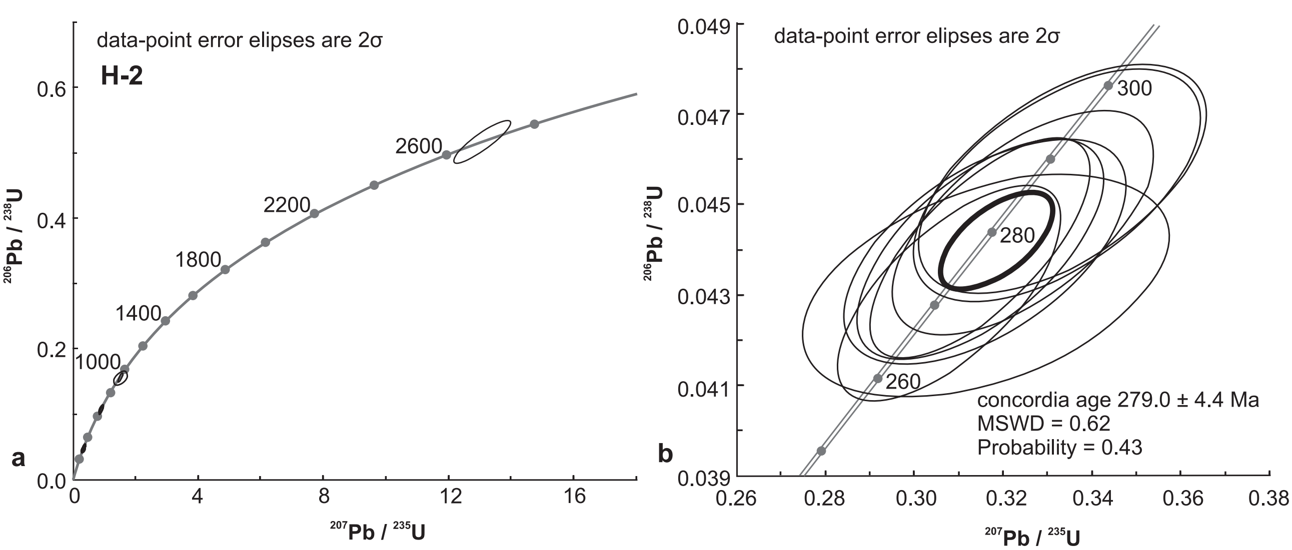

Fig. 7 Concordia plots showing the magmatic zircon ages from the sample *H-2,* and corresponding concordia age: **a** – all data (n = 14); **b** – detail on Permian ages (n = 8).

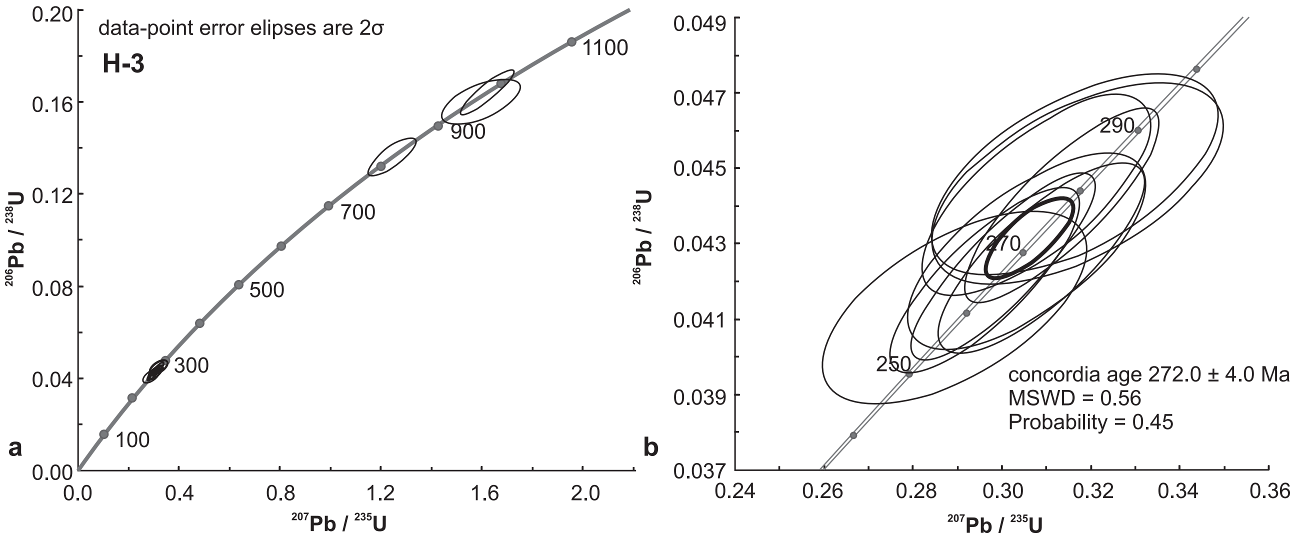

Fig. 8 Concordia plots showing the magmatic zircon ages from the sample *H-3,* and corresponding concordia age: **a** – all data (n = 12); **b** – detail on Permian ages (n = 9).

by opening of the Neotethys Ocean (Ziegler et al. 1997; Ziegler and Stampfli 2001; Stampfli and Borell 2002; Torsvik and Cocks 2004). These plate tectonic reconstructions show a continent–continent collision in the western and central European realms and at its southeastern edge a Paleotethys oceanic plate subduction towards the N and NW, beneath the Laurussia plate. According to the palaeotectonic reconstruction of Cassinis et al. (2012) for the Mediterranean region, the subduction of the Paleotethys oceanic ridge beneath the Eurasia margin created a triple junction and induced a progressive transformation of the Variscan chain from a convergent margin to a diffuse dextral transform margin, progressively affected by transtension and crustal thinning.

The progressive change of the collisional to dextral shear deformation is characteristic also of the Variscan Western Carpathians. The regional dextral shear movement was responsible for derivation of the uppermost Pennsylvanian and/or Cisuralian strike-slip and transtensional sedimentary basins. In general, alluvial-to-lacustrine continental deposition was coupled with a magmatic activity of sub-alkaline to weakly alkaline composition. From the paleogeographic point of view, the Late Palaeozoic sedimentary basins migrated with time from the SE to NW, i.e. from the current Internal to the Central Western Carpathians (Vozárová 1998).

The new U–Pb zircon ages from the HVH volcanic rocks enable dating the beginning of the Variscan post-orogenic sedimentation in the Northern Veporicum realm to the uppermost Cisuralian – Kungurian. The basal Brusno Fm. overlaps unconformably the Variscan crystalline basement that consists mostly of migmatites

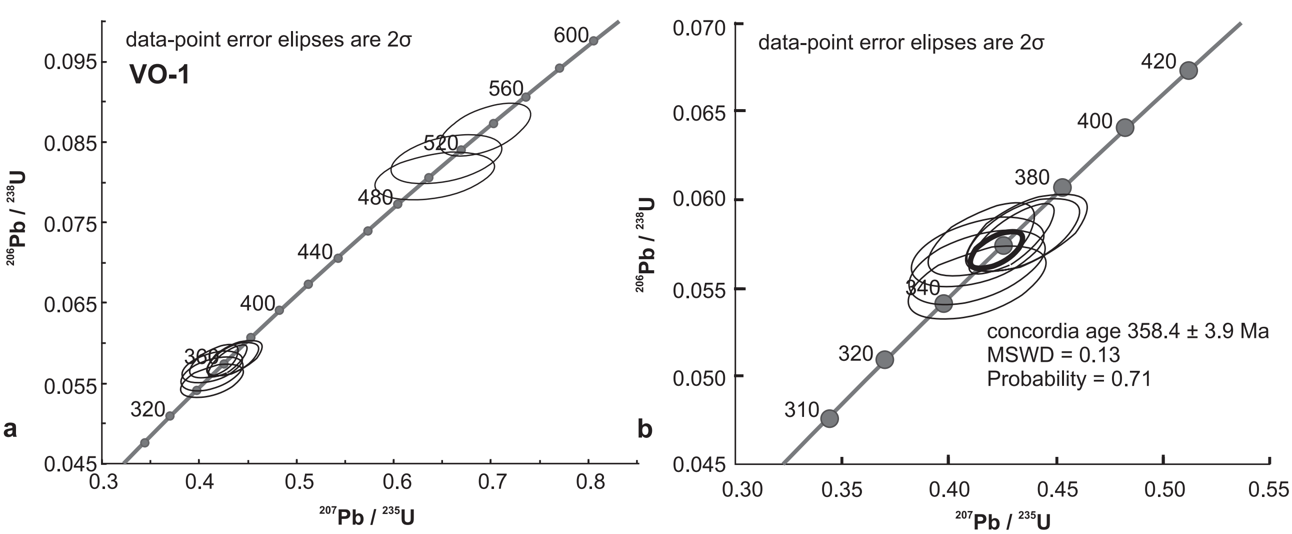

Fig. 9 Concordia plots showing the magmatic zircon ages from the sample *VO-1,* and corresponding concordia age: **a** – all data (n = 10); **b** – detail on Variscan age data (n = 7).

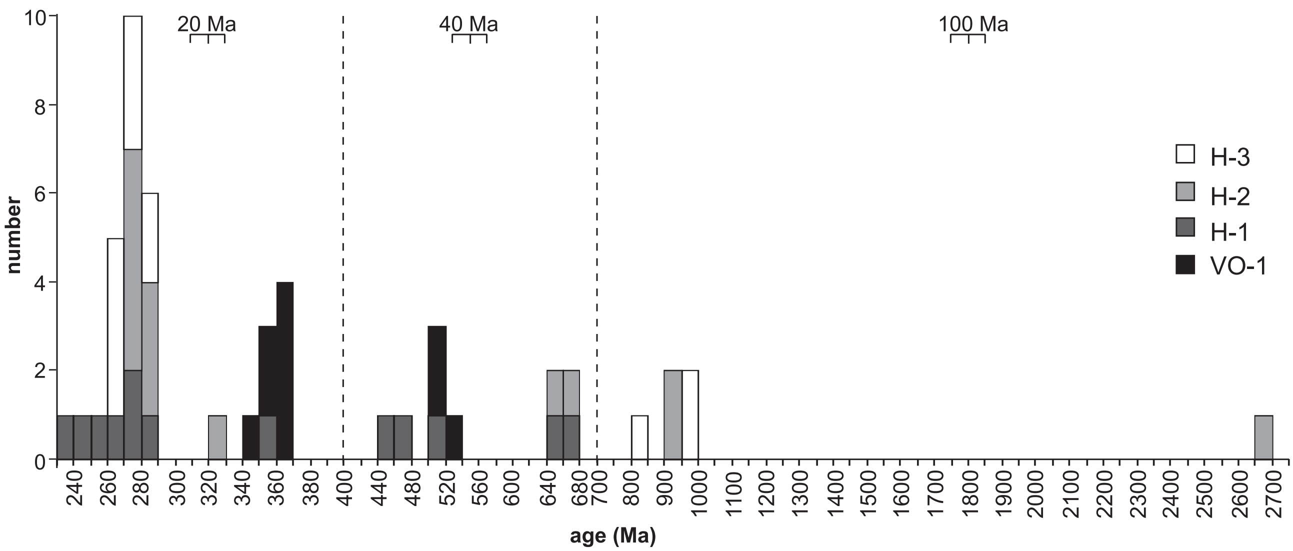

Fig. 10 Frequency histogram of the zircon $^{206}Pb/^{238}U$ ages from the HVH Permian volcanites, metatonalite and the intra-crystalline dyke including both magmatic and xenocrystic zircon ages.

and granitoid rocks. They were the supposed source for the Brusno Fm. deposits, as it is reflected in their arkosic composition (Vozárová 1979).

Strike-slip and normal faults were caused by the dextral shear movement and triggered Kungurian sedimentation in the Northern Veporicum sedimentary basin, and above that, largely wrecked underlying crystalline basement. Thus the HVH volcanic event was connected with the coeval system of volcanic and subvolcanic dykes with some small intrusions into the crystalline basement (Petrík et al. 1995; Bezák et al. 2008 and references therein). Bezák et al. (2008) documented 240 ± 22 Ma and 260 ± 12 Ma CHIME monazite ages from the trondhjemite body between Beňuš and Braväcovo villages, N of the Hron River. The origin of magma in the 283–249 Ma time range was confirmed also by the LA-ICP-MS zircon dating of the same authors. The 269 ± 9 Ma monazite isochron age of the granite porphyry from Osrblie clearly indicates the Guadalupian Epoch (Bezák at al. 2008). These data are near the Permian–Triassic LA-ICP-MS U–Pb zircon ages of 238.6 ± 1.4 Ma for the Hrončok granite by Putiš et al. (2000), as well as to 267 ± 2 Ma SHRIMP zircon age by Uher et al. (2008). Similarly, Permian ages were documented for the small acid intrusives at the southern slopes of the Kráľová hoľa Mt. (Finger et al. 2003; Gaab et al. 2005). This Permian plutonism was associated also with the low-grade metamorphism at 278 ± 5 and 275 ± 12 Ma (CHIME monazite dating) within the metapelitic members of the crystalline basement (Jeřábek et al. 2008).

The dextral shear tectonic regime gradually changed to an extensional during the Guadalupian and Lopingian and due to this, the magmatic activity was gradually continued and connected with a regional reheating. Evidence provide the above-mentioned Permian/Triassic isotopic magmatic ages (Bezák et al. 2008; Putiš et al. 2000), as well as in the newly obtained zircon age of 244 ± 6 Ma for the sample *H-1* indicative of diffusion and/or fluid-driven dissolution–reprecipitation with the Pb-loss.

Distinct change in the tectonic regime is documented by the gap in sedimentation between the Brusno and Predajná formations. It reflects a structural rearrangement of the sedimentary basin, i.e. a change of transport directions and depocentres, as well as the later reworking of the HVH volcanic rocks as well as fragments from the intra-crystalline volcanic dykes into the basal conglomerates of the Predajná Fm. (Vozárová 1979).

The exact durations of the sedimentation and stratigraphic gap between the Brusno and Predajná formations is uncertain, due to the lack of biostratigraphic markers. The overlying Lower Triassic sediments rest upon the different lithological horizons of the Predajná Fm. unconformably (Vozárová 1979). The intra-Permian disconformity between both formations was most likely caused by a deformation pulse, which induced faulting, uplift and erosion or break in sedimentation. It can be related to the so-called "Mid-Permian Episode" of Deroin and Bonin (2003) and may have been synchronous with the Guadalupian geomagnetic "Illawara Reversal" event (Menning 1995, 2001). The two regional sedimentary cycles within the post-Variscan sequences were described in the Eastern Alps (Krainer 1993; Vozárová et al. 2009b and references therein), in the Southern Alps as well as in the peri-Mediterranean realm (Cassinis et al. 2012 and references therein). Generally it is considered that the Guadalupian–Lopingian tectonic event was linked to the substantial plate reorganisation, leading to the opening of the Neotethys Ocean (Ziegler and Stampfli 2001; Vai 2003; Muttoni et al. 2009; Cassinis et al. 2012) and the Pangaea breakup (Isozaki 2009).

In contrast, the 358 ± 4 Ma zircon age from the metatonalites of the Volchovo Valley (sample *VO-1*) is quite consistent with the zircon magmatic ages from the Vepor Pluton (Gaab et al. 2005; Kohút et al. 2008). The pebbles of metavolcanic rocks, cataclastically deformed microgranites as well as tourmaline-bearing rocks and tourmalinites were found in the basal conglomerates of the Predajná Fm. (Vozárová-Minarovičová 1966; Vozárová 1979). This material could have been derived from the retrogressed crystalline basement.

8. Conclusions

Dacites/trachyandesites from the Harnobis Volcanogenic Horizon of the Brusno Fm. sequence yielded 273 and 279 Ma (Kungurian) ages. These volcanic rocks were contemporaneous with sedimentation of the associated Brusno Fm. arkoses verifying that the Northern Veporicum Permian sedimentary basin was established during the latest Kungurian, and was one of the latest compared to other dextral-shearing-related Permian basins of the Western Carpathians.

Intrusion of magmatic dykes to the crystalline basement was coeval with sedimentation in the Northern Veporicum Permian basin, as documented by the 272 Ma zircon age of the trachyandesite dyke from the Kelemen's tunnel. The reworking of the volcanic lenses and volcanic dykes to the basal conglomerates of the overlying Predajná Fm. indicates a break in sedimentation and a stratigraphic gap at Guadalupian.

From the geochemical point of view, the studied Kungurian volcanic and sub-volcanic rocks have a weak alkaline character with an affinity to continental within-plate tectonic setting.

Based on the *c.* 358 Ma zircon age, the metatonalite (sample *VO-1*) is time equivalent of the Variscan Vepor Pluton. The studied rock shows a calk-alkaline character with the affinity to an active continental margin tectonic setting.

Acknowledgements: The financial support of the Slovak Research and Development Support Agency (project ID: APVV-0546-11) and VEGA (project VEGA 1/0141/15) is gratefully acknowledged. The authors would like to thank M. Putiš and M. Tichomirowa for constructive reviews which led to significant improvement of this manuscript. We are also grateful to M. Kohút and V. Janoušek for their useful comments and for careful editing of the manuscript.

References

Andrusov D (1968) Grundriss der Tectonic der Nördlichen Karpaten. Slovenská Akadémia Vied, Bratislava, pp 1–187

Andrusov D, Bystrický J, Fusán O (1973) Outline of Geological Structure of the West Carpathians. Guidebook, X Congress Carpatho–Balkan Geological Association. Dionýz Štúr Geological Institute, Bratislava, pp 5–44

Bajaník Š, Biely A, Miko O, Planderová E (1979) About Paleozoic volcanic-sedimentary Predná Hola Complex (Nízke Tatry Mts.). Geol Práce, Spr 73: 7–28 (in Slovak)

Balogh K, Kovach Á (1973) Determination of the Battonya quartz porphyries age by Rb/Sr method. ATOMKI Közl 15: 245–249 (in Hungarian)

Bezák V, Broska I, Konečný P, Petrík I, Košler J (2008) Permian magmatic complex in Northern Veporicum: interpretation of new datings of acid magmatites. Miner Slov 40: 127–134 (in Slovak with English summary)

Biely A, Bezák V, Elečko M, Gross P, Kaličiak M, Konečný V, Lexa J, Mello J, Nemčok J, Potfaj M, Rakús M, Vass D, Vozár J, Vozárová A (1996a) Explanation to geological map of Slovakia, 1 : 500 000. Dionýz Štúr Publishers, Bratislava, pp 1–232 (in Slovak with English summary)

Biely A, Bezák V, Elečko M, Gross P, Kaličiak M, Konečný V, Lexa J, Mello J, Nemčok J, Potfaj M, Rakús M, Vass D, Vozár J, Vozárová A (1996b) Geological map of Slovakia, 1 : 500 000. Ministry of the Environment of Slovak Republic, Geological Survey of Slovak Republic, Bratislava

Black LP, Kamo SL, Allen CM, Aleinikoff JN, Davis DW, Korsch RJ, Foudoulis C (2003) TEMORA 1: a new zircon standard for Phanerozoic U–Pb geochronology. Chem Geol 200: 155–170

Bleahu M, Lupu M, Patrulius D, Bordea S, Ştefan A, Panin S (1981) The Structure of the Apuseni Mountains. Guide to Excursion B 3. XII Congress Carpatho–Balkan Geological Association. Institute of Geology and Geophysics, Bucharest, pp 1–103

Broska I, Petrík I, Be′eri-Schlevin Y, Majka J, Bezák V (2013) Devonian–Mississippian I-type granitoids in the Western Carpathians: a subduction-related hybrid magmatism. Lithos 162–163: 27–36

Cassinis G, Perotti CR, Ronchi A (2012) Permian continental basins in the Southern Alps (Italy) and Peri-Mediterranean correlations. Int J Earth Sci 101: 129–157

Corfu F, Hanchar JM, Hoskin PWO, Kinny P (2003) Atlas of zircon textures. In: Hanchar JM, Hoskin PWO (eds) Zircon. Mineralogical Society of America and Geochemical Society, Reviews in Mineralogy and Geochemistry 53: 469–500

Cortesogno L, Cassinis G, Dallagiovanna G, Gaggero L, Oggiano G, Ronchi A, Seno S, Vanossi M (1998) The

Variscan post-collisional volcanism in Late Carboniferous–Permian sequences of Ligurian Alps, Southern Alps and Sardinia (Italy): a synthesis. Lithos 45: 305–328

Cortesogno L, Gaggero L, Ronchi A, Yanev S (2004) Late orogenic magmatism and sedimentation within Late Carboniferous to Early Permian basins in the Balkan Terrane (Bulgaria): geodynamic implications. Int J Earth Sci 93: 500–520

Deroin JP, Bonin B (2003) Late Variscan tectonomagmatic activity in Western Europe and surroundings areas: thin Mid-Permian Episode. Bull Soc Geol It Spec Vol 2: 169–184

Digital Geological Map of Slovakia 1 : 50 000. Accessed on December 1, 2015, at *http://mapserver.geology.sk/gm50js/*

Finger F, Broska I, Haunschmid B, Hraško L, Kohút M, Krenn E, Petrík I, Riegler G, Uher P (2003) Electron-microprobe dating of monazites from Western Carpathians basement granitoids: plutonic evidence for an important Permian rifting event subsequent to Variscan crustal anatexis. Int J Earth Sci 92: 86–98

Gaab AS, Poller U, Janák M, Kohút M, Todt W (2005) Zircon U–Pb geochronology and isotopic characterization for the pre-Mesozoic basement of the Northern Veporic Unit (Central Western Carpathians, Slovakia). Schweitz Mineral Petrogr Mitt 85: 69–88

Gorton MP, Schandl ES (2000) From continents to island arcs: a geochemical index of tectonic setting for arc-related and within-plate felsic to intermediate volcanic rocks. Canad Mineral 38: 1065–1073

Hanchar JM, Miller CF (1993) Zircon zonation patterns as revealed by cathodoluminescence and back-scattered electron imaging to dating zircons from lower crustal xenoliths. Chem Geol 110: 1–13

Ilavský J, Vozárová A, Vozár J (1994) Ľubietová: structural boreholes LU-1, LU-2 and LU-3. Region Geol Západ Karpát 29: 1–77 (in Slovak)

International Stratigraphic Chart (2014) International Subcommission on Stratigraphy. Accessed on July 28, 2016 at *http://www.stratigraphy.org/ICSChart/ChronostratChart2014-10.pdf*

Isozaki Y (2009) Illawara Reversal: the fingerprint of superplume that triggered Pangean breakup and the end-Guadalupian (Permian) mass extinction. Gondwana Res 15: 421–432

Jaroš J (1969) Setting of the Root Zone of the Krížná Nappe in the West Carpathians. Čas Mineral Geol 14: 141–149

Jeřábek P, Janák M, Faryad SW, Finger F, Konečný P (2008) Polymetamorphic evolution of pelitic schists and evidence for Permian low-pressure metamorphism in the Vepor Unit, West Carpathians. J Metamorph Geol 26: 465–485

Kamenický J (1968) Some problems of the West Carpathians crystalline complex. Geol Zborn Slov Akad Vied 19: 7–20

Kamenický J (1977) Der geologische Bau des Nordwestlichen Teiles der Vepor-Erzgebirges. Acta geol geogr Univ Comen 32: 5–43

Klinec A (1976) Geological map of Slovenské Rudohorie (middle part) and Nízke Tatry Mts. (eastern part), 1 : 50 000., Dionýz Štúr Geological Institute, Bratislava

Klinec A, Vozár J (1971) Discussion to tectonic evolution of Veporic crystalline rock complexes, Choč Unit and so-called Heľpa Mesozoic sequence. Geol Práce, Spr 56: 221–226 (in Slovak)

Klötzli US, Mair V, Bargossi GM (2003) The "Bozener Quartzporphyr" (Southern Alps, Italy): single zircon U/Pb age evidence for 10 million years of magmatic activity in the Lower Permian. Mitt Österr mineral Gesell 148: 187–188

Kohút M, Frank W, Petro M (2000) The Sparistá Dolina granitic mylonites: the products of the Alpine deformation. Slovak Geol Mag 6: 347–361

Kohút M, Uher P, Putiš M, Sergeev S, Antonov A (2008) Dating of Early Carboniferous granitic rocks of the Western Carpathians: based on SHRIMP U–Pb zircon ages. Miner Slov 40: 204 (in Slovak)

Kohút M, Trubač J, Novotný L, Ackerman L, Demko R, Bartalský B, Erban V (2013) Geology and Re–Os molybdenite geochronology of the Kurišková U–Mo deposit (Western Carpathians, Slovakia). J Geosci 58: 275–286

Korikovsky SP, Miko O (1992) Low-grade metasediments of the Kraklová Formation of Veporic Crystalline Complex. Miner Slov 24: 381–391 (in Slovak)

Korikovsky SP, Putiš M, Plašienka D (1997) Cretaceous low-grade metamorphism of the Veporic and North-Gemeric zones: a result of collisional tectonics in the central Western Carpathians. In: Grecula P, Hovorka D, Putiš M (eds) Geological Evolution of the Western Carpathians. Miner Slov, Monograph. Geocomplex, Bratislava, pp 107–130

Kotov AB, Miko O, Putiš M, Korikovsky SP, Saľnikova EB, Kovach VP, Yakovleva SZ, Bereznaya NG, Kráľ J, Krist E (1996) U/Pb dating of zircons of postorogenic acid metavolcanics and metasubvolcanics: a record of Permian–Triassic taphrogeny of the West-Carpathian basement. Geol Carpath 47: 73–79

Kozur H, Mock R (1973) Zum Alter und zur tektonische Stellung der Meliata Serie des Slowakische Karstes. Geol Zborn Slov Akad Vied 24: 364–374

Kozur H, Mock R (1995) First evidence of Jurassic in the Folkmar Suture Zone of the Meliaticum in Slovakia and its tectonic implications. Miner Slov 27: 301–307

Kozur H, Mock R (1997) New paleogeographic and tectonic interpretation in the Slovakian Carpathians and their implications for correlations with the Eastern Alps. Part II. Inner Western Carpathians. Miner Slov 29: 164–209

Krainer K (1993) Late- and Post-Variscan sediments in the Eastern and Southern Alps. In: von Raumer JF, Neubauer

F (eds) Pre-Mesozoic Geology in the Alps. Springer, Berlin, pp 537–564
Kräutner HG (1997) Alpine and pre-Alpine terranes in the Romanian Carpathians and Apuseni Mts. Ann géol Pays hellén 37: 331–400
Krstić B, Karamata S (1992) Terranes of the Serbian Carpatho–Balkanides. Compt Rend Seanc Soc Serb Geol, livre jubilaire (1891–1991), Belgrade: 57–74
Kubíny D (1959) Report to geological mapping in surrounding of the Heľpa. Geol Práce, Spr 17: 143–176 (in Slovak)
Larionov AN, Andreichev VA, Gee DG (2004) The Vendian alkaline igneous suite of northern Timan: ion microprobe U–Pb zircon ages of gabbros and syenite. In: Gee DG, Pease VL (eds) The Neoproterozoic Timanide Orogen of Eastern Baltica. Geological Society of London, Memoirs 30: 69–74
Ludwig KR (2005a) SQUID 1.12, A User's Manual. A Geochronological Toolkit for Microsoft Excel. Berkeley Geochronology Center, Special Publications, pp 1–22
Ludwig KR (2005b) User's Manual for Isoplot/Ex 3.22. A Geochronological Toolkit for Microsoft Excel. Berkeley Geochronology Center, Special Publications, pp 1–71
Maheľ M (ed) (1964) Explanation to Geological Map of Czechoslovakia, 1 : 200 000. Czech Geological Survey, Prague, pp 1–270
Maheľ M (1986) Geological structure of the Czechoslovak Carpathians, Part 1: Paleoalpine Units. Veda, Bratislava, pp 1–503 (in Slovak)
Maheľ M, Buday T (eds) (1968) Regional Geology of Czechoslovakia. Part II. The West Carpathians. Academia, Prague, pp 1–495
McCann T, Kiersnowski H, Krainer K, Vozárová A, Peryt TM, Opluštil S, Stollhofen H, Schneider J, Wetzel A, Boulvain F, Dusar M, Török Á, Haas J, Tait J, Körner F (2008) Permian. In: McCann (ed) The Geology of Central Europe, Vol. 1: Precambrian and Palaeozoic. Geological Society of London, pp 531–597
McDonough WF, Sun SS (1995) The composition of the Earth. Chem Geol 120: 223–253
Menning M (1995) A numerical time scale 2000 for the Permian and Triassic period: an integrated time analysis. In: Sholle PA, Peryt TM, Ulmer Sholle DS (eds) The Permian of Northern Pangea Vol 1. Springer, Berlin, pp 77–97
Menning M (2001) A Permian time scale 2000 and correlation of marine and continental sequences using the Illawara Reversal (265 Ma). In: Cassinis G (ed) Permian Continental Deposits of Europe and Other Areas. Regional Reports and Correlations. Natura Bresciana, Ann Mus Civ Sci Nat, Monografia 25: 355–362
Miko O (1981) Middle Palaeozoic sedimentary-volcanic sequence of the Jánov Grúň in the Veporicum crystalline basement of the Nízke Tatry Mts. Geol Zborn Geol Carpath 32: 465–474 (in Russian)
Mišík M, Chlupáč I, Cicha I (1985) Stratigraphic and Historic Geology. SPN, Bratislava, pp 1–570 (in Slovak)
Muttoni G, Gaetani M, Kent DV, Sciunnach D, Angiolini L, Berra F, Garzanti E, Mattei M, Zanchi A (2009) Opening of the Neo-Tethys Ocean and the Pangea B to Pangea A transformation during the Permian. GeoArabia 14: 17–47
Nelson ST, Montana A (1992) Sieve-textured plagioclase in volcanic rocks produced by rapid decompression. Amer Miner 77: 1242–1249
Nicolae I, Seghedi I, Boboș I, Rosário Azevedo M, Ribeiro S, Tatu M (2014) Permian volcanic rocks from the Apuseni Mountains (Romania): geochemistry and tectonic constrains. Chem Erde 74: 125–137
Pearce JA (1983) The role of sub-continental lithosphere in magma genesis of destructive plate margins. In: Hawkesworth CJ, Norry MJ (eds) Continental Basalts and Mantle Xenoliths. Shiva, Nantwich, pp 230–249
Petrík I. Broska I, Bezák V, Uher P (1995) Hrončok type granite – Hercynian A-type granite in the shear zone. Miner Slov 27: 351–364 (in Slovak)
Planderová E, Miko O (1977) New datings of Veporic crystalline rocks based on palynomorph analysis. Miner Slov 9: 275–292 (in Slovak)
Plašienka D (1998) Paleotectonic evolution of the Central Western Carpathians during the Jurassic and Cretaceous. In: Rakús M (ed) Geodynamic Development of the Western Carpathians. Geological Survey of the Slovak Republic, Bratislava, pp 107–130
Plašienka D, Grecula P, Putiš M, Kováč M, Hovorka D (1997) Evolution and structure of the Western Carpathians: an overview. In Grecula P, Hovorka D, Putiš M (eds) Geological Evolution of the Western Carpathians. Miner Slov Monograph. Geocomplex, Bratislava, pp 1–24
Polák M (ed) (2003) Geological map of the Starohorské vrchy Mts., Čierťaž Mts. and northern part of Zvolenská Kotlina Depression, 1:50 000. Ministry of Environment of the Slovak Republic – State Dionýz Štúr Geological Institute, Bratislava
Poller U, Huth Y, Hoppe P, Williams IS (2001) REE, U, Th and Hf and Hf distributions in zircon from Western Carpathians Variscan granitoids: a combined cathodoluminescence and ion microprobe study. Amer J Science 301: 858–876
Putiš M (1991) Tectonic styles and Late Variscan–Alpine evolution of Tatric–Veporic crystalline basement in the Western Carpathians. Zbl Geol Paläont, Teil I Vol 1: 181–204
Putiš M, Kotov AB, Uher P, Saľnikova JB, Korikovsky SP (2000) Triassic age of the Hrončok pre-orogenic A-type granite related to continental rifting: a new result of U–Pb isotope dating (Western Carpathians). Geol Carpath 51: 59–66

Putiš M, Sergeev S, Ondrejka M, Larionov A, Siman P, Spišiak J, Uher P, Paderin I (2008) Cambrian–Ordovician metaigneous rocks associated with Cadomian fragments in the West-Carpathian basement dated by SHRIMP on zircons: a record from the Gondwana active margin setting. Geol Carpath 59: 3–18

Putiš M, Frank W, Plašienka D, Siman P, Sulák M, Biroň A (2009a) Progradation of the Alpidic Central Western Carpathian orogenic wedge related to subductions: constrained by $^{40}Ar/^{39}Ar$ ages of white micas. Geodin Acta 22: 31–56

Putiš M, Ivan P, Kohút M, Spišiak J, Siman P, Radvanec M, Uher P, Sergeev S, Larionov A, Méres S, Demko R, Ondrejka M (2009b) Meta-igneous rocks of the West-Carpathian basement, Slovakia: indicators of Early Paleozoic extension and shortening events. Bull Soc Géol France 180: 461–471

Rojkovič I, Konečný P (2005) Th–U–Pb dating of monazite from the Cretaceous uranium vein mineralization in the Permian rocks of the Western Carpathians. Geol Carpath 56: 493–502

Rudnick RL, Fountain DM (1995) Nature and composition of the continental crust – a lower crustal perspective. Rev Geophys 33: 267–309

Seghedi A, Popa M, Oaie G, Nicolae I (2001) The Permian system in Romania. Natura Bresciana, Ann Mus Civ Sci Nat, Monografia 25: 281–293

Stacey JS, Kramers JD (1975) Approximation of terrestrial lead isotope evolution by a two-stage model. Earth Planet Sci Lett 26: 207–221

Stampfli GM, Borel GD (2002) A plate tectonic model for Paleozoic and Mesozoic constrained by dynamic plate boundaries and restored synthetic oceanic isochrons. Earth Plan Sci Lett 196: 17–33

Stan N (1984) Contribution to the mineralogical and petrochemical study of the ignimbritic rocks from the Codru-Moma Mts. (Apuseni Mts.). D S Inst Geol Geofiz 68: 221–232

Stan N (1987) Upper Carboniferous and Permian volcanism from Romania. In: Flügel HW, Sassi FP, Grecula P (eds) Pre-Variscan and Variscan Events in the Alpine-Mediterranean Belt. Miner Slov, Monograph. Alfa, Bratislava, pp 445–456

Sun SS, McDonough WF (1989) Chemical and isotope systematic of oceanic basalts: implications for mantle composition and processes. In: Saunders AD, Norry MJ (eds) Magmatism in Ocean Basins. Geological Society of London, Special Publications 42: 313–345

Torsvik TH, Cocks LRM (2004) Earth geography from 400 to 250 Ma: a paleomagnetic, faunal and facies review. J Geol Soc, London 161: 255–572

Uher P. Putiš M, Ondrejka M, Kohút M, Sergeev S (2008) Post-orogenic A-type granites in the Western Carpathians: result of the SHRIMP zircon dating. Miner Slov 40: 204–205 (in Slovak)

Vai GB (2003) Development of the palaeography of Pangaea from Late Carboniferous to Early Permian. Palaeogr Plaoclimat Palaeoecol 196: 125–155

Vozár J (1965) Metamorphic Mesozoic rocks in the western part of the Veporides. Geol Práce, Spr 35: 33–40 (in Slovak)

Vozár J (1979) Contribution to structural position and correlation of the envelope series in the northern part of the Veporicum. Geol Práce, Spr 72: 19–30 (in Slovak)

Vozárová-Minarovičová A (1966) Discovery of tourmaline-bearing rock pebbles in the Ľubietová Permian conglomerates. Geol Práce, Spr 40: 165–167 (in Slovak)

Vozárová A (1979) Lithofacial characteristics of Permian in NW part of Veporicum. Západné Karpaty, Sér Min Petr Geoch Metalog 6: 61–116 (in Slovak with English summary)

Vozárová A (1998) Late Carboniferous to Early Permian time interval in the Western Carpathians: Northern Tethys margin. In: Crasquin-Soleau S, Izart A, Vaslet D, De Wever P (eds) Peri-Tethys: Stratigraphic Correlations, Vol. 2. Geodiversitas 20: 621–641

Vozárová A, Vozár J (1988) Late Palaeozoic in West Carpathians (Mladšie paleozoikum v Západných Karpatoch). Geologický ústav Dionýza Štúra, Bratislava, pp 1–214 (in English and in Slovak)

Vozárová A, Konečný P, Vozár J, Šmelko M (2008) Upper Jurassic–Lower Cretaceous tectonothermal events in the Southern Gemeric Permian rocks deduced from electron microprobe dating of monazite. Geol Carpath 59: 89–102

Vozárová A, Šmelko M, Paderin I (2009a) Permian single crystal U–Pb zircon age of the Rožňava Formation volcanites (Southern Gemeric Unit, Western Carpathians, Slovakia). Geol Carpath 60: 439–448

Vozárová A, Ebner F, Kovács S, Kräutner HG, Szederkenyi T, Krstić B, Sremac J, Aljinović D, Novak M, Skaberne D (2009b) Late Variscan (Carboniferous to Permian) environments in the Circum Pannonian Region. Geol Carpath 60: 71–104

Vozárová A, Šmelko M, Paderin I, Larionov A (2012) Permian volcanics in the Northern Gemericum and Bôrka Nappe system: U–Pb zircon dating and implication to geodynamic evolution (Western Carpathians, Slovakia). Geol Carpath 63: 191–200

Vozárová A, Konečný P, Šarinová K, Vozár J (2014) Ordovician and Cretaceous tectonothermal history of the Southern Gemericum Unit from microprobe monazite geochronology (Western Carpathians, Slovakia). Int J Earth Sci 103: 1005–1022

Vozárová A, Presnyakov S, Šarinová K, Šmelko M (2015) First evidence for Permian–Triassic boundary volcanism in the Northern Gemericum: geochemistry and U–Pb zircon geochronology. Geol Carpath 66: 375–391

Wiedenbeck M, Alleé P, Corfu F, Griffin Wl, Meier M, Oberli F, von Quadt A, Roddick JC, Spiegel W (1995)

Three natural zircon standards for U–Th–Pb, Lu–Hf, trace element and REE analyses. Geostand Newsl 19: 1–23
Williams IS (1998) U–Th–Pb geochronology by ion microprobe. In: McKibben MA, Shanks WC, Ridley WI (eds) Applications in Microanalytical Techniques to Understanding Mineralizing Processes. Rev Econ Geol 7: 1–35
Winchester JA, Floyd PA (1977) Geochemical discrimination of different magma series and their differentiation products using immobile elements. Chem Geol 20: 325–343
Ziegler PA, Stampfli GM (2001) Late Palaeozoic–Mesozoic plate boundary reorganization: collapse of the Variscan orogeny and opening of Neotethys. In: Cassinis G (ed) Permian Continental Deposits of Europe and Other Areas: Regional Reports and Correlations. Natura Bresciana, Ann Mus Civ Sci Nat, Brescia, Monografia 25: 17–34
Ziegler AM, Hulver ML, Rowley DB (1997) Permian world topography and climate. In: Martiny IP (ed) Late Glacial and Post-Glacial Environmental Changes: Quaternary, Carboniferous–Permian and Proterozoic. Oxford Univ Press, Oxford, pp 111–146
Zoubek V (1936) Remarks to the crystalline basement of the Western Carpathians. Věst St Geol Úst Čs Republ 12: 207–239 (in Czech)
Zoubek V (1957) Report about geological researches in Vepor Mts near Brusno. Zpr geol Výzk v r 1956: 197–200 (in Czech)